

**Top 2023**

**Traverse City, US**

**September 24-29, 2023**



**Measurement of differential cross sections in  $t\bar{t}$  and  $t\bar{t}+\text{jets}$  production in the  $\ell+\text{jets}$  decay mode in  $pp$  collisions at  $\sqrt{s} = 13 \text{ TeV}$  using  $140 \text{ fb}^{-1}$  of ATLAS data**

**Claudia Glasman**

**Universidad Autónoma de Madrid**

**on behalf of the ATLAS Collaboration**



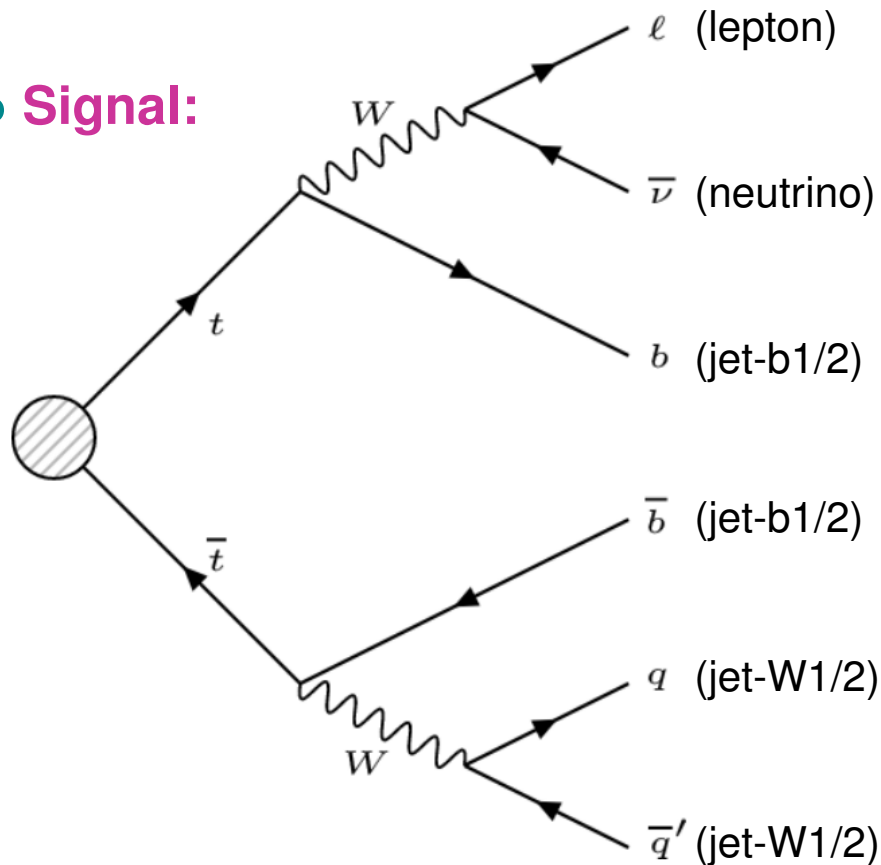
# $t\bar{t}$ differential cross sections in the $\ell$ +jets decay mode



- **Measurements of  $t\bar{t}$  and  $t\bar{t}$ +jets differential cross sections**
  - $pp$  collisions at  $\sqrt{s} = 13$  TeV using  $140 \text{ fb}^{-1}$
  - absolute and normalised cross sections at particle level in  $\ell$ +jets decay mode
  - jet observables in three channels:  $t\bar{t}$  inclusive,  $t\bar{t} + 1\text{jet}$  and  $t\bar{t} + 2\text{jets}$
  - comparison of measurements with NLO and NNLO QCD predictions
- **Motivation:**
  - characterization of the kinematics and topology of the  $t\bar{t}$  system ( $t\bar{t}$  inclusive channel) via transverse momentum and rapidity of jets and their angular correlations
  - characterization of the kinematics, dynamics and topology of the hardest ( $t\bar{t} + 1\text{jet}$  channel) and second-hardest ( $t\bar{t} + 2\text{jets}$  channel) QCD emissions via transverse momentum and rapidity of jets and their angular correlations and invariant masses
  - tests of pQCD theory via NLO and NNLO predictions

# $t\bar{t}$ signal and background

- **Signal:**



- **Signature for  $\ell$ +jets  $t\bar{t}$  processes:**

- **charged lepton**
- **neutrino**
- **two bottom quarks**
- **two jets with invariant mass closest to  $m_W$**

- **Signature for the  $t\bar{t} + 1$ jet channel:**

- **at least one additional jet**

- **Signature for the  $t\bar{t} + 2$ jets channel:**

- **at least two additional jets**

- **Additional jets can arise from ISR and/or FSR**

highest (second-highest)  $p_T$  additional jet arising from hard QCD radiation: 'jet-rad1/2'

- **Background (simulated using MC samples):  $\approx 10\%$  in each channel**

- **single top,  $W$ +jets, multijets (data-driven method),  $Z$ +jets,  $t\bar{t}V$ , diboson,  $t\bar{t}H$**

# Fiducial phase space and QCD predictions



## Fiducial phase space (particle level)

- exactly one lepton ( $e$  or  $\mu$ ) with  $p_T > 27$  GeV and  $|\eta| < 2.5$
- at least 4 jets (2 ghost-matched with a  $B$ -hadron) with  $p_T > 25$  GeV and  $|y| < 2.5$
- overlap removal: if  $\Delta R(\ell, \text{jet}) < 0.4$ ,  $\ell$  is removed

## ● QCD predictions:

- **NLO**: PWG+PY8, PWG+HW7, aMC@NLO+HW7 and SHERPA 2.2.12 (using NNPDF3.0(N)NLO)
- **NNLO (in  $t\bar{t}$  system)**: PWG+PY8 MiNNLOPS (using NNPDF3.0NNLO)
- **Normalisation from Top++2.0 at NNLO+NNLL with  $m_t = 172.5$  GeV**:  

$$\sigma_{t\bar{t}} = 832_{-29}^{+20} \text{ (scale)} \pm 35 \text{ (PDF, } \alpha_s) \pm 23 \text{ (} m_t) \text{ pb}$$
- **Theoretical uncertainties: scale variations, PDFs and  $\alpha_s$** 
  - **scale variations dominant**:  $\approx 10\%$  ( $\approx 40\%$ ) at low (high)  $p_T$  at NLO  
 $\approx 5\%$  ( $\approx 10\%$ ) at low (high)  $p_T$  at NNLO
  - further reduction for normalised cross sections



# Observables I

- Observables in  $t\bar{t}$  inclusive ( $N^{\text{jets}} \geq 4$ , no additional jets explicitly requested)

→ transverse momenta of jets:

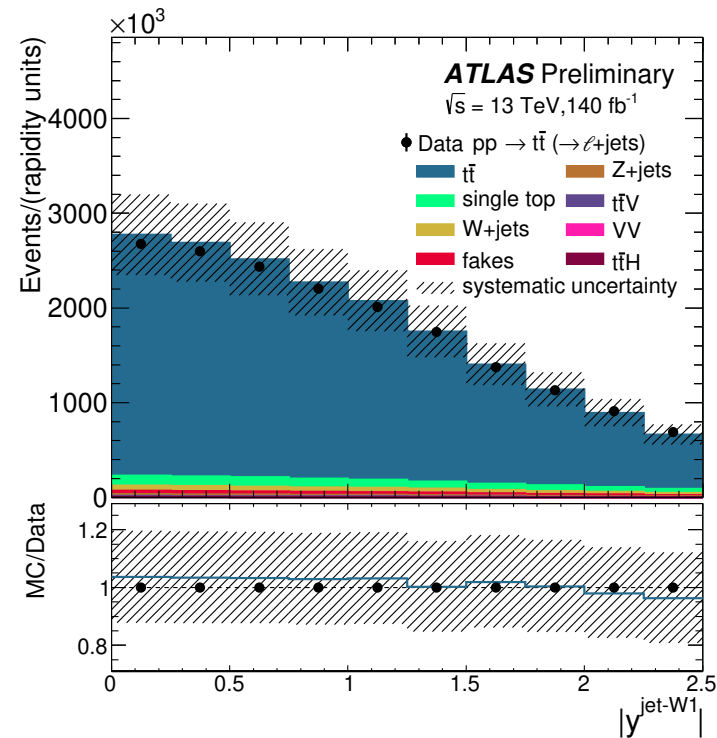
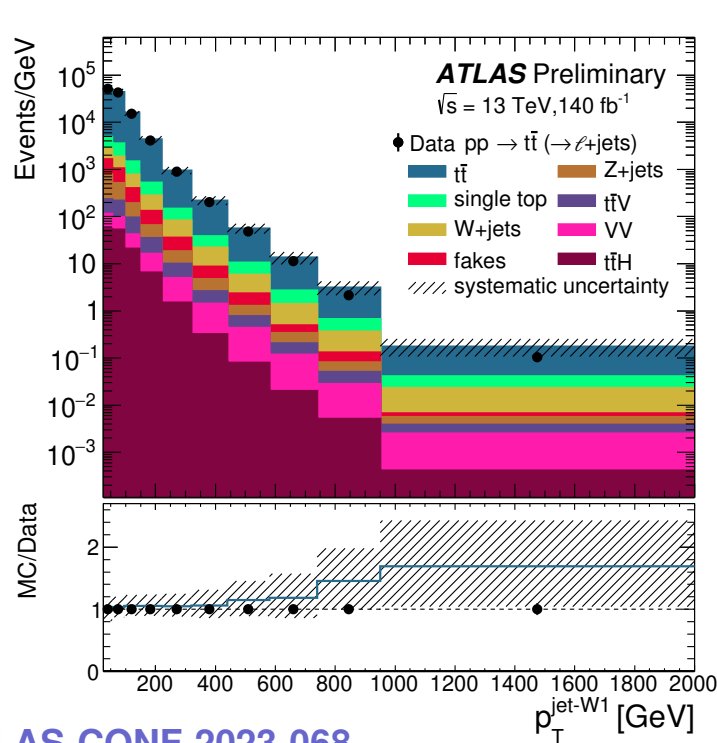
$$p_T^{\text{jet-W1}} \text{ and } p_T^{\text{jet-W2}}$$

→ angular correlations:

$$|\Delta y^{\text{jet-W1} - \text{jet-W2}}| \text{ and } |\Delta \phi^{\text{jet-W1} - \text{jet-W2}}|$$

→ rapidities of jets:

$$|y^{\text{jet-W1}}| \text{ and } |y^{\text{jet-W2}}|$$



# Observables II

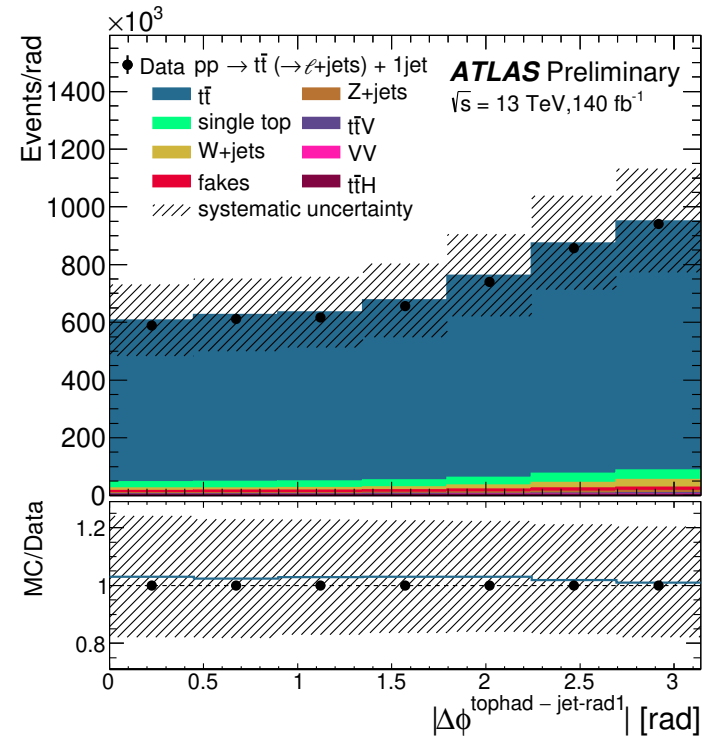
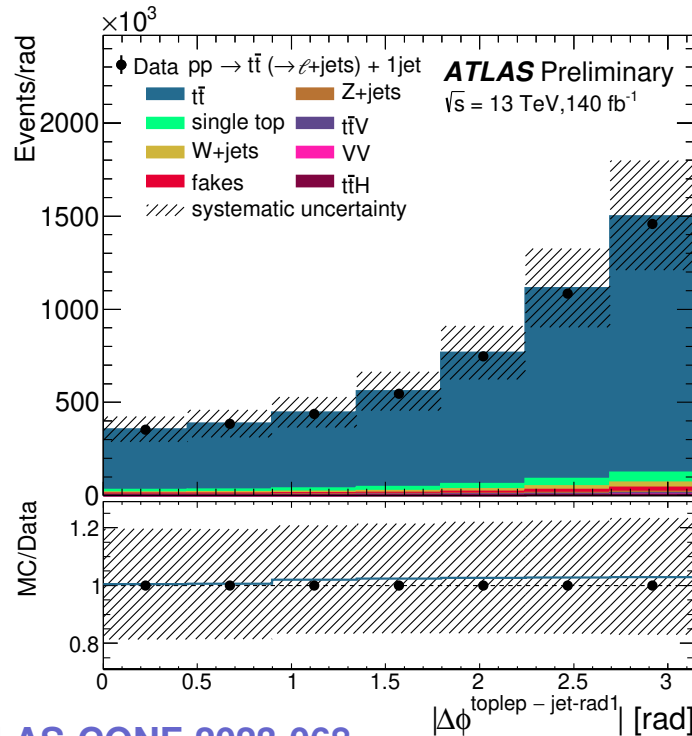
- **Observables in  $t\bar{t}+1$  jet ( $N^{\text{jets}} \geq 5$ , one additional jet explicitly requested)**

→ **transverse momentum and rapidity of additional jet:**  $p_T^{\text{jet-rad1}}$   $|y^{\text{jet-rad1}}|$

→ **angular correlations:**

$|\Delta\phi^{\text{jet-W1-jet-rad1}}|$ ,  $|\Delta\phi^{\text{tolep-jet-rad1}}|$  and  $|\Delta\phi^{\text{tophad-jet-rad1}}|$

→ **invariant mass:**  $m^{t\bar{t}-\text{jet-rad1}}$

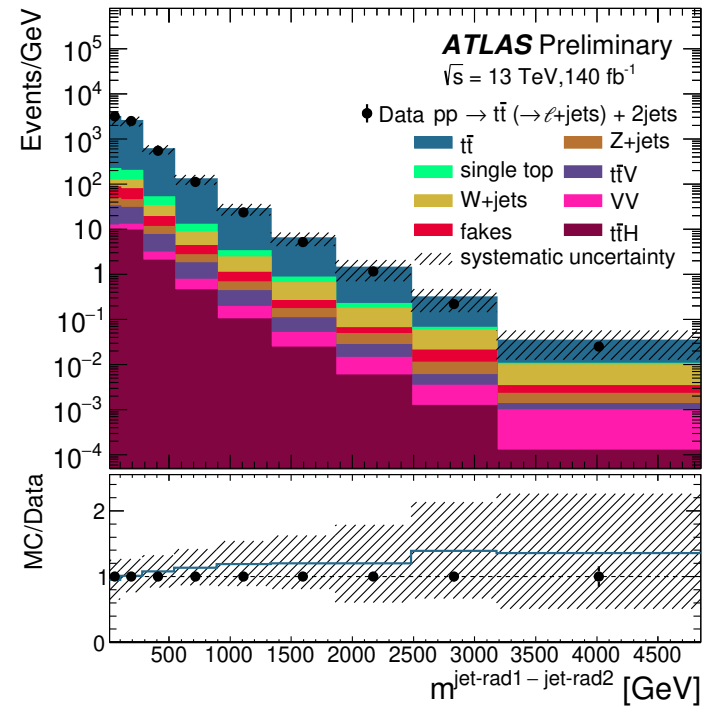
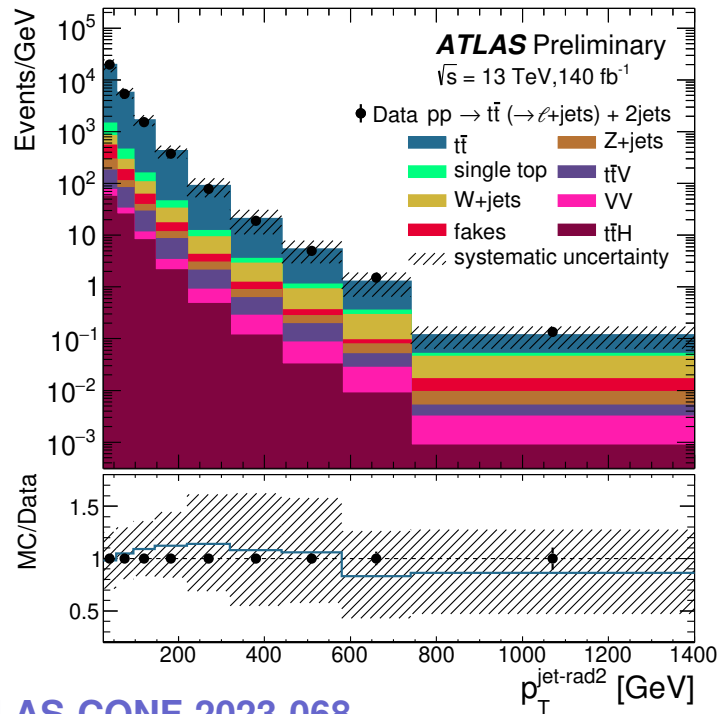




# Observables III

● Observables in  $t\bar{t}+2$  jets ( $N^{\text{jets}} \geq 6$ , two additional jets explicitly requested)

- transverse momentum and rapidity of additional jet:  $p_T^{\text{jet-rad2}}$  and  $|y^{\text{jet-rad2}}|$
- angular correlations:  $|\Delta y^{\text{jet-rad1} - \text{jet-rad2}}|$ ,  $|\Delta \phi^{\text{jet-rad1} - \text{jet-rad2}}|$ ,  $|\Delta \phi^{\text{toplep} - \text{jet-rad2}}|$ ,  $|\Delta \phi^{\text{tophad} - \text{jet-rad2}}|$  and  $|\Delta \phi^{\text{jet-W1} - \text{jet-rad2}}|$
- invariant mass:  $m^{\text{jet-rad1} - \text{jet-rad2}}$



# Unfolding

- The data distributions, after background subtraction, were unfolded using the iterative application of Bayes theorem with 2 iterations to obtain the measured differential cross sections at particle level using unfolding matrices with detector- and particle-level objects which are angularly well matched (to suppress combinatorial background)

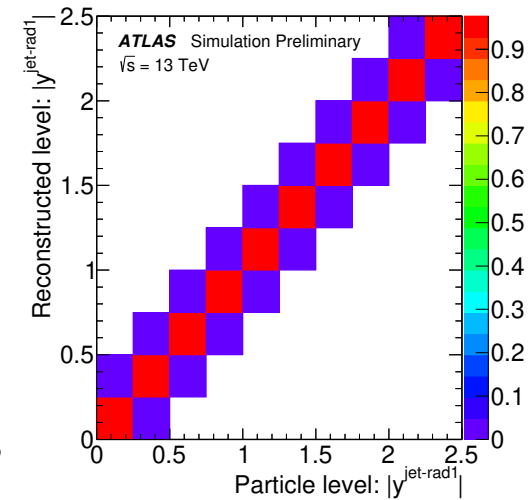
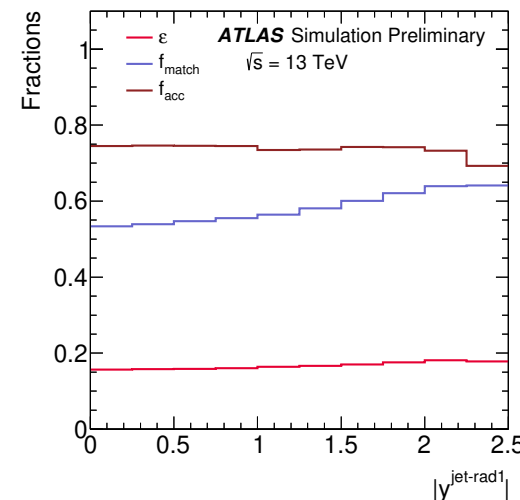
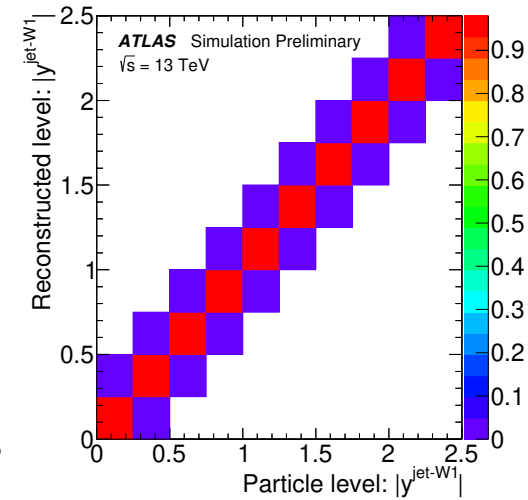
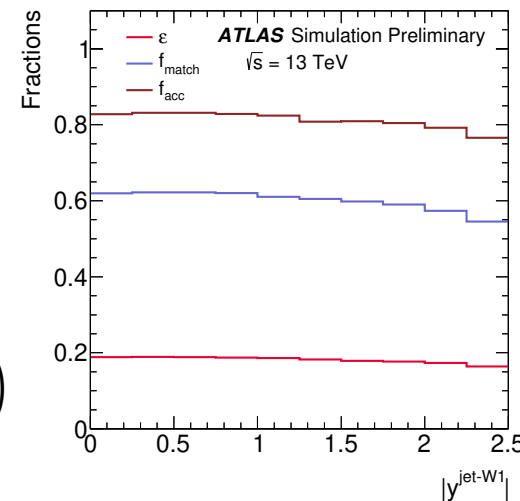
$$\frac{d\sigma}{dX_i} \equiv \frac{1}{\mathcal{L} \cdot \Delta X_i} \cdot N_i^{\text{unf}}$$

$$N_i^{\text{unf}} \equiv \frac{1}{\epsilon^i} \cdot \sum_j f_{\text{match}}^j \cdot \mathcal{M}_{ij}^{-1} \cdot f_{\text{acc}}^j \cdot (N_{\text{detector}}^j - N_{\text{bkg}}^j)$$

$$f_{\text{acc}}^j = \frac{N_{\text{particle} \wedge \text{detector}}^j}{N_{\text{detector}}^j}$$

$$f_{\text{match}}^j = \frac{N_{\text{particle} \wedge \text{detector} \wedge \text{match}}^j}{N_{\text{particle} \wedge \text{detector}}^j}$$

$$\epsilon^i = \frac{N_{\text{particle} \wedge \text{detector}}^i}{N_{\text{particle}}^i}$$







# Systematic uncertainties

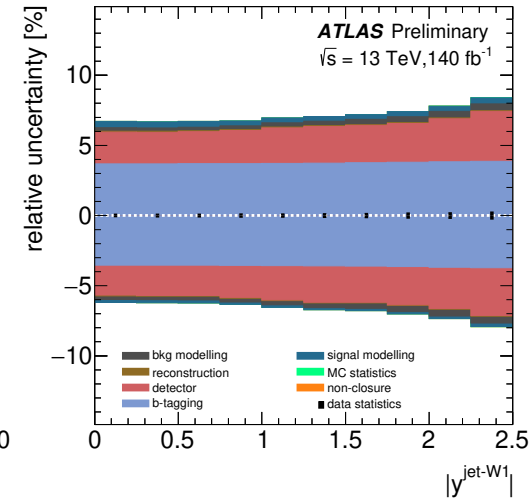
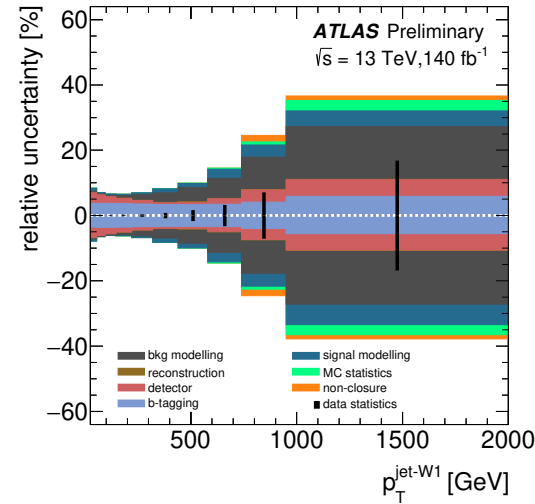
● The following sources of systematic uncertainties were considered:

- $b$ -tagging calibration and efficiency
- detector energy scale and resolution
- reconstruction efficiency
- background modelling
- signal modelling
- non-closure
- statistics
- (luminosity →  $\pm 0.83\%$ )

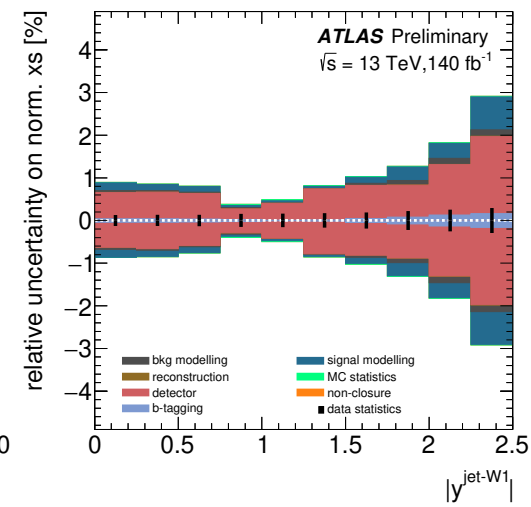
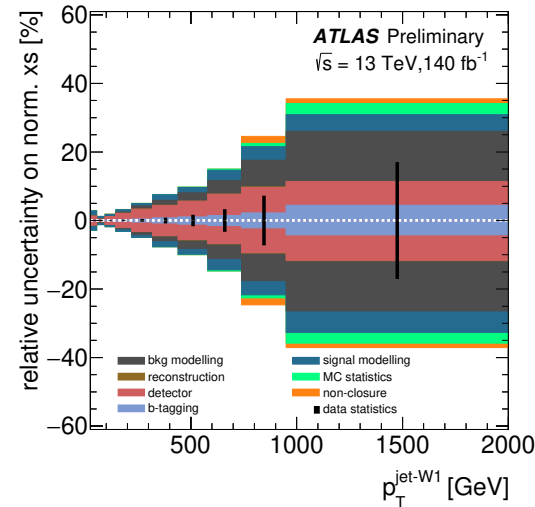
● Total relative uncertainty:

- $\approx 7\%$  ( $\approx 1\%$ ),  $\approx 10\%$  ( $\approx 1.5\%$ ) and  $\approx 13\%$  ( $\approx 2\%$ ) for  $t\bar{t}$  inclusive,  $t\bar{t} + 1\text{jet}$  and  $t\bar{t} + 2\text{jets}$  at low  $p_T$  for absolute (normalised) cross sections

## absolute cross sections



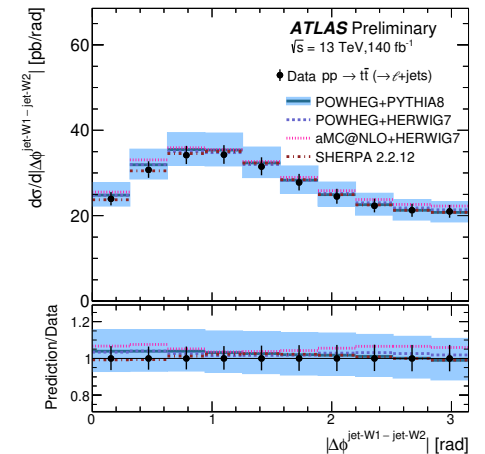
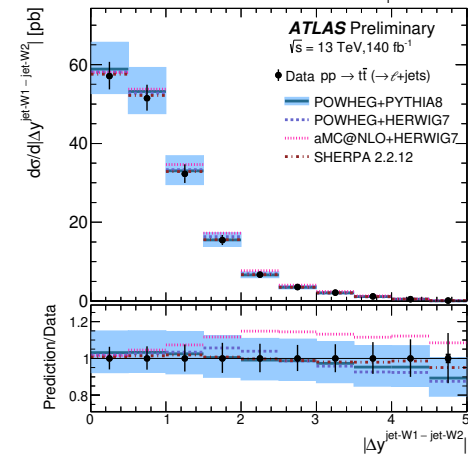
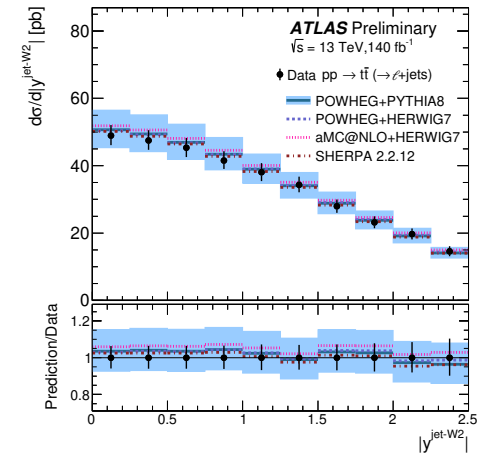
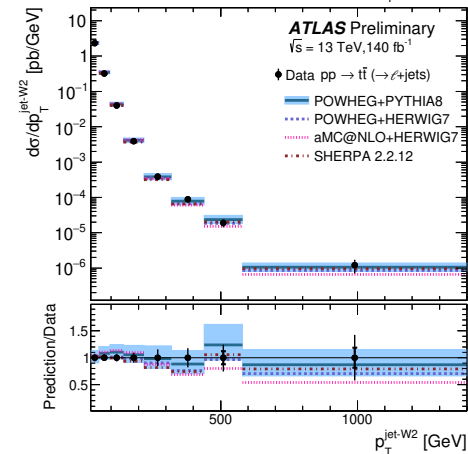
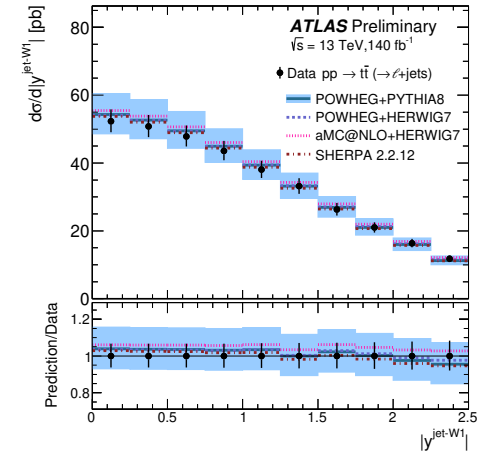
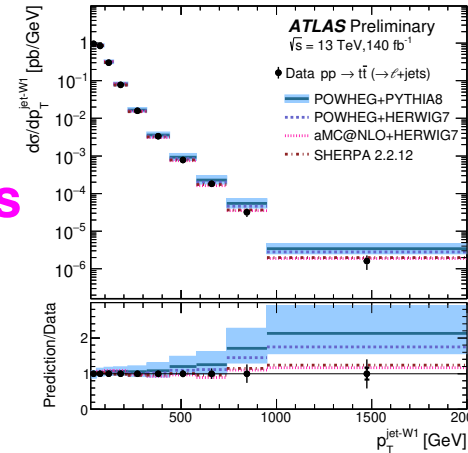
## normalised cross sections





# Results

- **Absolute differential cross sections for  $t\bar{t}$  inclusive channel vs NLO:**
- **Motivation:** characterization of kinematics and topology of  $t\bar{t}$  system
- **Measured cross section as a function of  $p_T^{\text{jet-W1}}$  has a harder spectrum than that of  $p_T^{\text{jet-W2}}$**
- **Measured cross sections as functions of  $|y^{\text{jet-W1}}|$  and  $|y^{\text{jet-W2}}|$  have very similar shape and normalisation**
- **Comparison with NLO QCD predictions:**
  - good description of angular observables
  - good description of  $p_T^{\text{jet-W1}}$  by SHERPA and aMC@NLO+Hw7
  - $p_T^{\text{jet-W2}}$  is in general well described

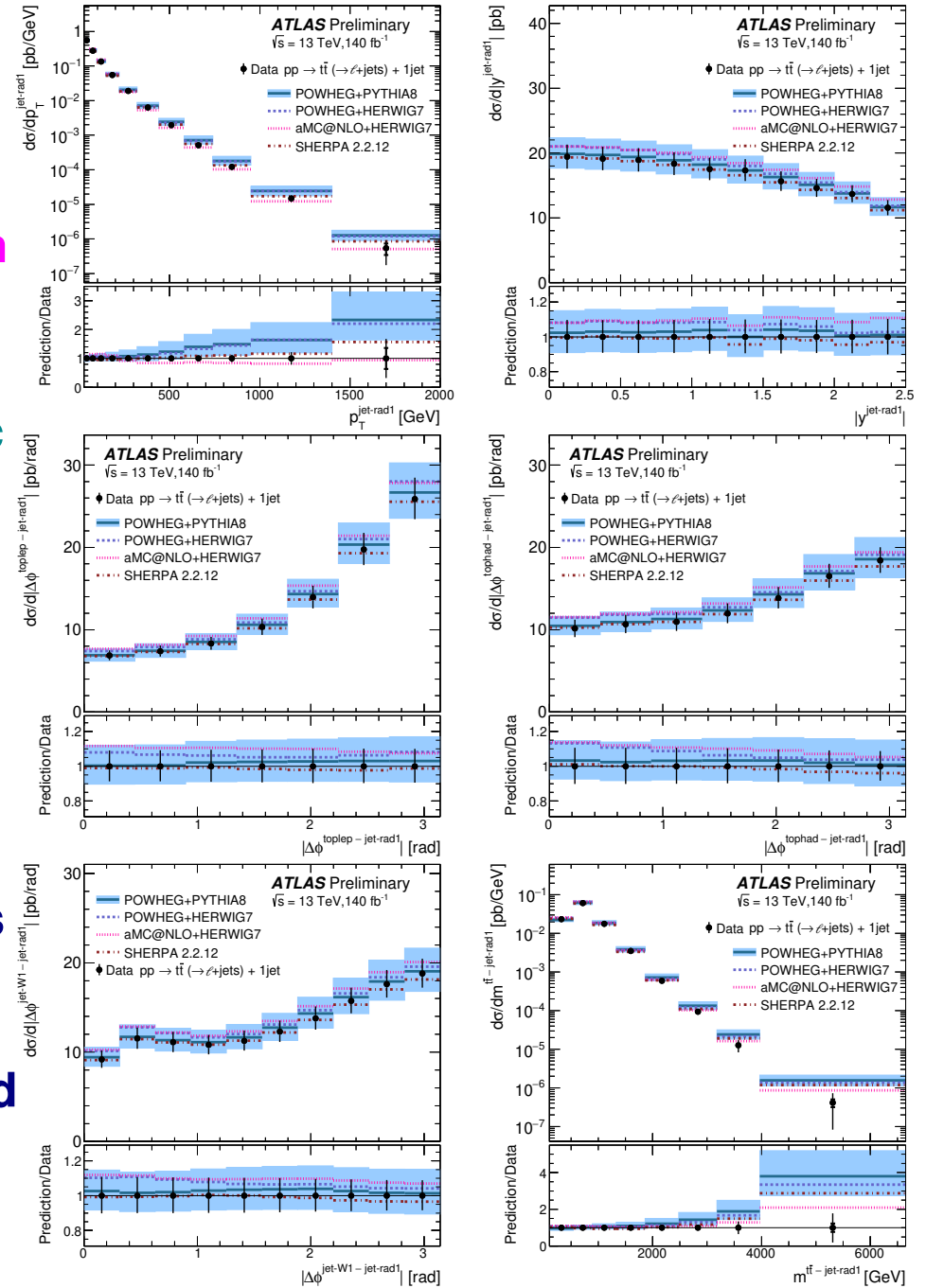




# Results

- **Absolute differential cross sections for  $t\bar{t}+1$  jet channel vs NLO:**
- **Motivation:** characterization of kinematics, dynamics and topology of hardest emission
- **Measured cross section as a function of  $|y^{\text{jet-rad1}}|$  is different than that of  $|y^{\text{jet-W1}}|$**   
 → first emission tends to be more isotropic than the jets forming the tophad
- **Measured cross sections as functions of  $|\Delta\phi^{\text{toplep-jet-rad1}}|$  and  $|\Delta\phi^{\text{tophad-jet-rad1}}|$  have different shapes**  
 → the hard radiation tends to be farther in  $\phi$  from the toplep than from the tophad
- **Comparison with NLO QCD predictions:**
  - good description of angular observables
  - good description of  $p_T^{\text{jet-rad1}}$  by SHERPA and aMC@NLO+Hw7
  - $m^{\text{t}\bar{t}-\text{jet-rad1}}$  is in general well described by aMC@NLO+Hw7

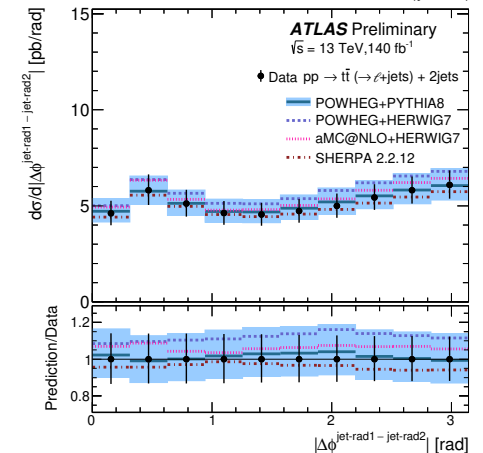
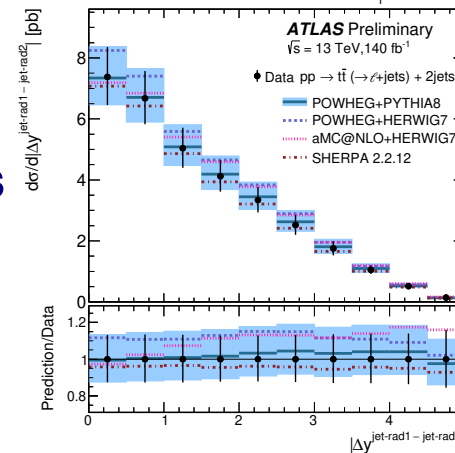
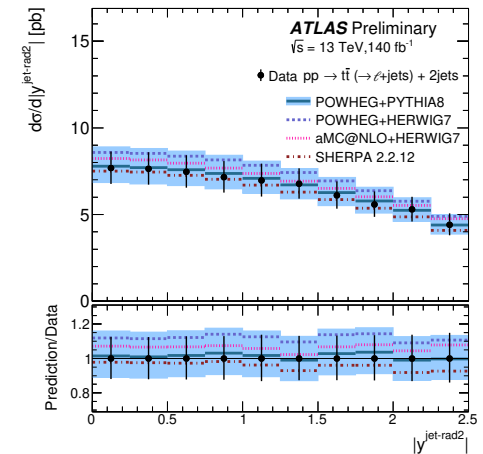
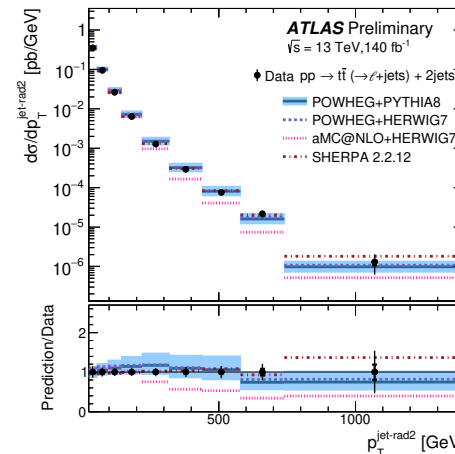
ATLAS Collab, ATLAS-CONF-2023-068





# Results

- **Absolute differential cross sections for  $t\bar{t}+2$  jets channel vs NLO:**
- **Motivation:** characterization of kinematics, dynamics and topology of second hardest emission
- **Measured cross section as a function of  $|y^{\text{jet-rad2}}|$  is different than that of  $|y^{\text{jet-W1}}|$**   
 → second emission tends to be more isotropic than the jets forming tophad
- **$|\Delta y^{\text{jet-rad1} - \text{jet-rad2}}|$  has different shape than  $|\Delta y^{\text{jet-W1} - \text{jet-W2}}|$**
- **$|\Delta \phi^{\text{jet-rad1} - \text{jet-rad2}}|$  has different shape than  $|\Delta \phi^{\text{jet-W1} - \text{jet-W2}}|$**
- **Comparison with NLO QCD predictions:**  
 → good description of angular observables  
 → good description of  $p_T^{\text{jet-rad2}}$  by SHERPA and POWHEG

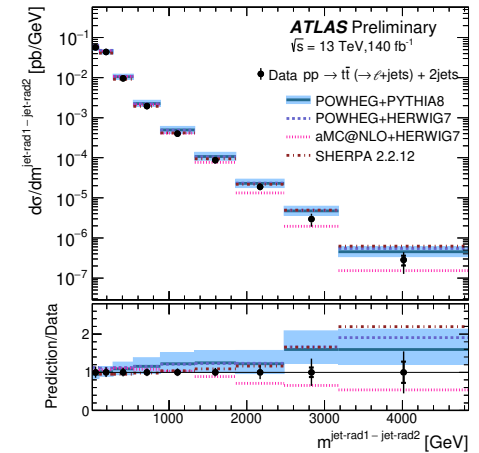
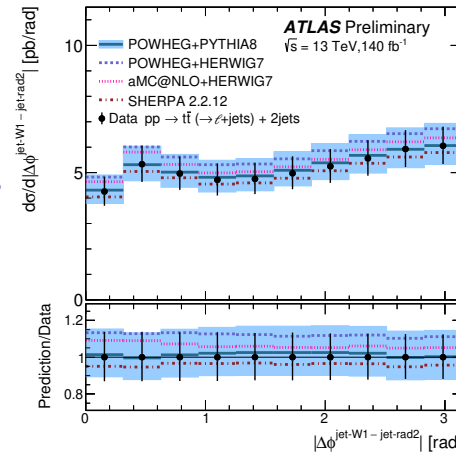
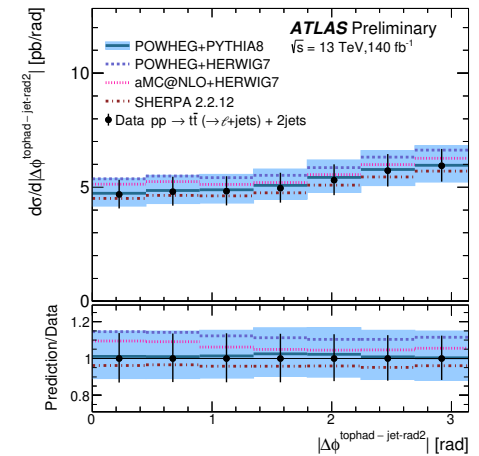
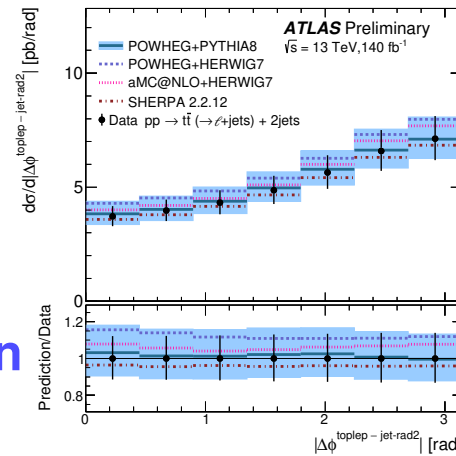


# Results

- Absolute differential cross sections for  $t\bar{t}+2$  jets channel vs NLO:
- Motivation: characterization of kinematics, dynamics and topology of second-hardest emission

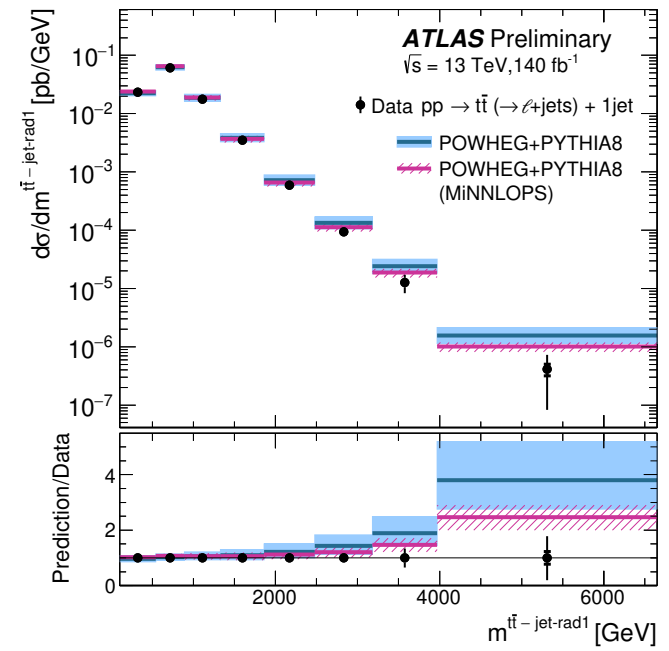
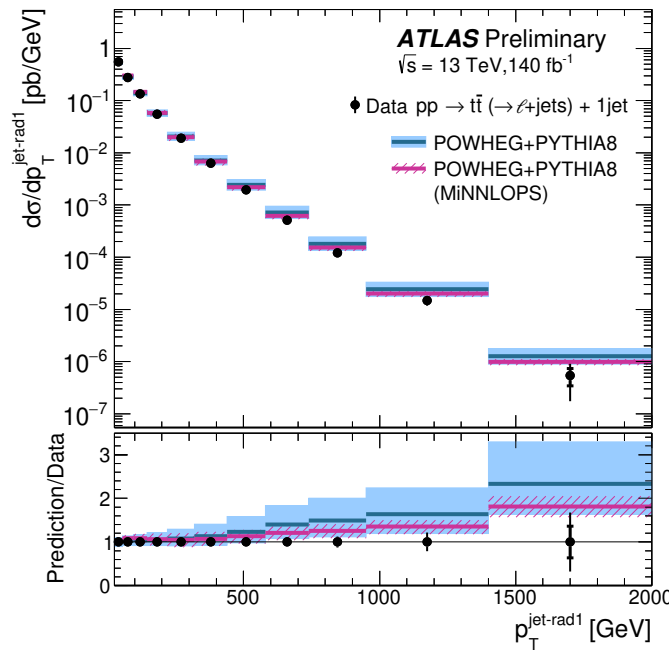
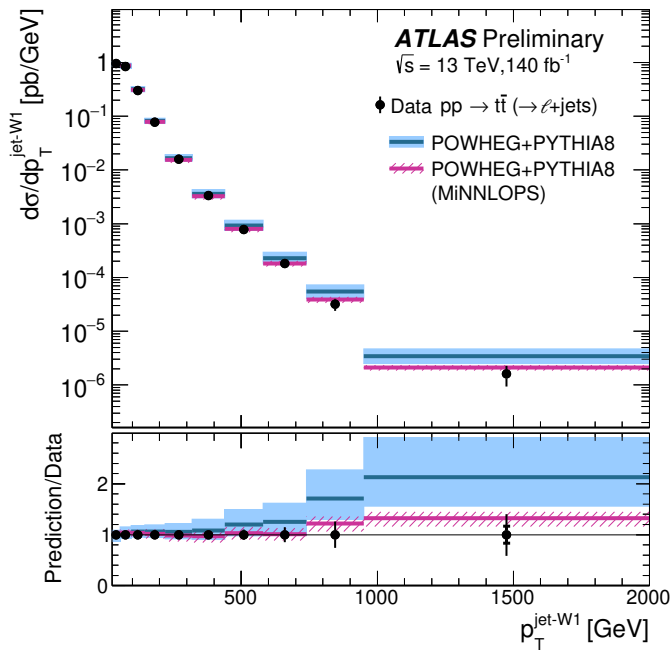
- Measured cross sections as functions of  $|\Delta\phi^{\text{tolep}} - \text{jet-rad2}|$  and  $|\Delta\phi^{\text{tophad}} - \text{jet-rad2}|$  have different shapes  $\rightarrow$  the hard radiation tends to be farther in  $\phi$  from the tolep than from the tophad and more isotropic than for first emission

- Comparison with NLO QCD predictions:  $\rightarrow$  good description of angular observables  $\rightarrow$  good description of  $m^{\text{jet-rad1} - \text{jet-rad2}}$  by SHERPA and POWHEG



# Results

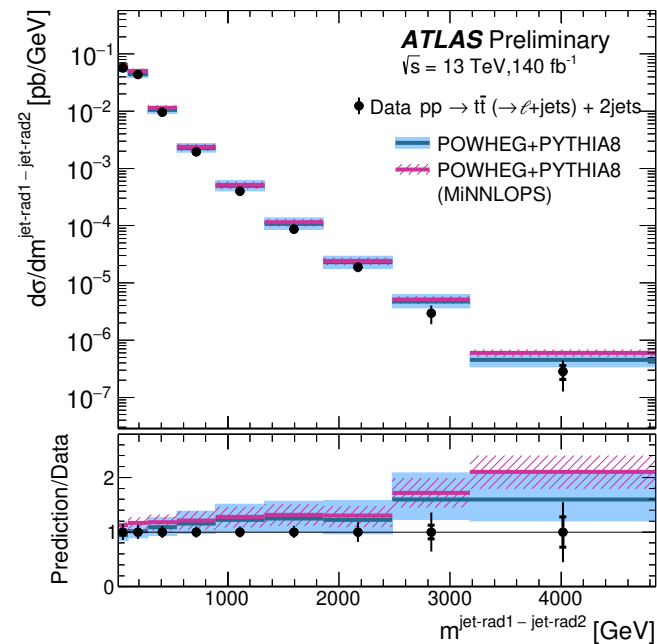
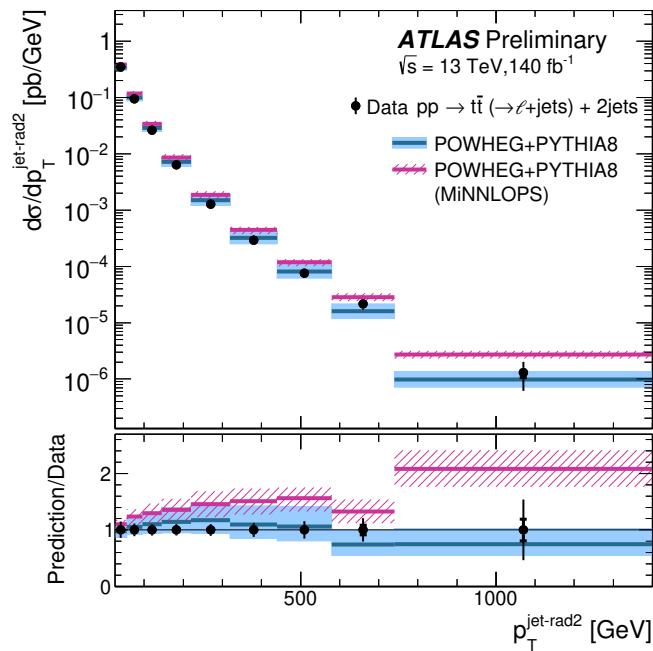
● Absolute differential cross sections vs NLO and NNLO:



⇒ Improved description of the  $p_T^{\text{jet-W1}}$ ,  $p_T^{\text{jet-rad1}}$  and  $m^{t\bar{t} - \text{jet-rad1}}$  measured cross sections by the NNLO predictions from PWG+Py8 MINNLOPS

# Results

## ● Absolute differential cross sections vs NLO and NNLO:



⇒ Description of  $p_T^{jet-rad2}$  and  $m^{jet-rad1 - jet-rad2}$  measured cross sections by NNLO does not improve

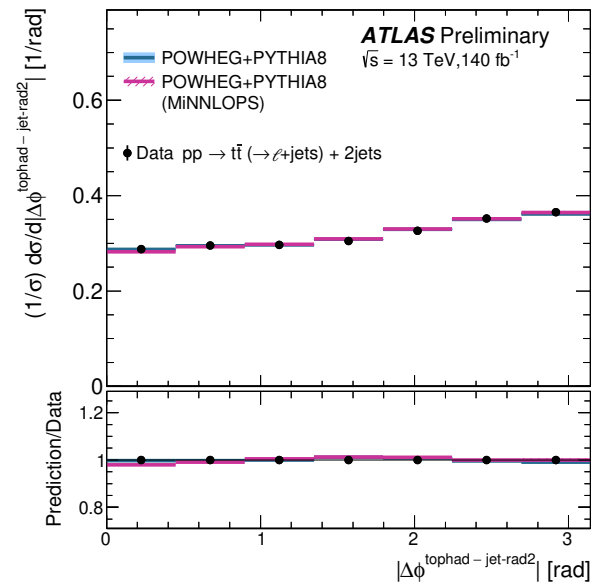
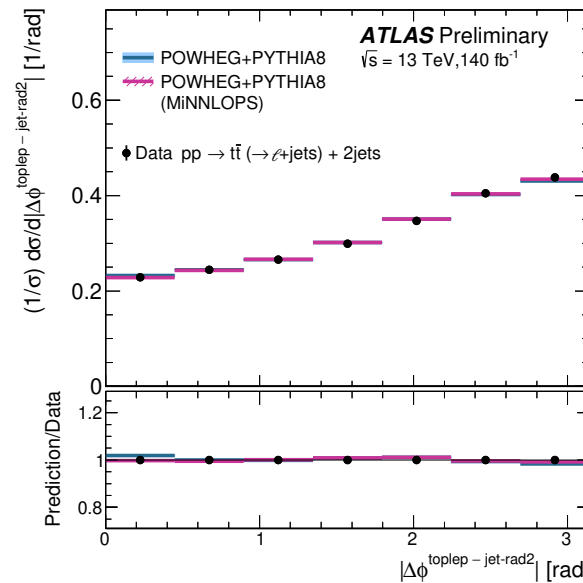
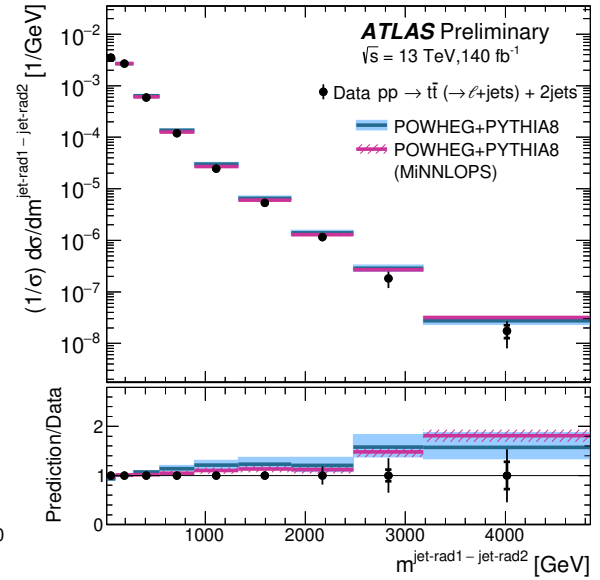
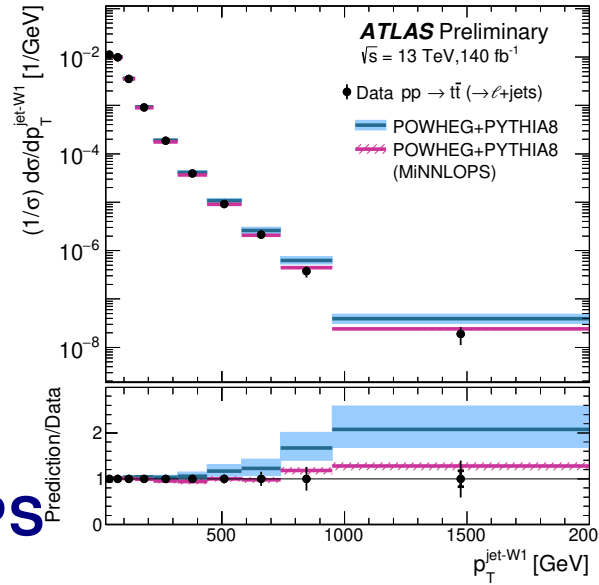
→ PWG+PY8 MINNLOPS prediction is only lowest order for second emission



# Results

- Some normalised differential cross sections vs NLO and NNLO:
- ⇒ Reduction of experimental and theoretical uncertainties

⇒ Good description of measured normalised differential cross sections by PWG+PY8 MINNLOPS with reduced theoretical and experimental uncertainties



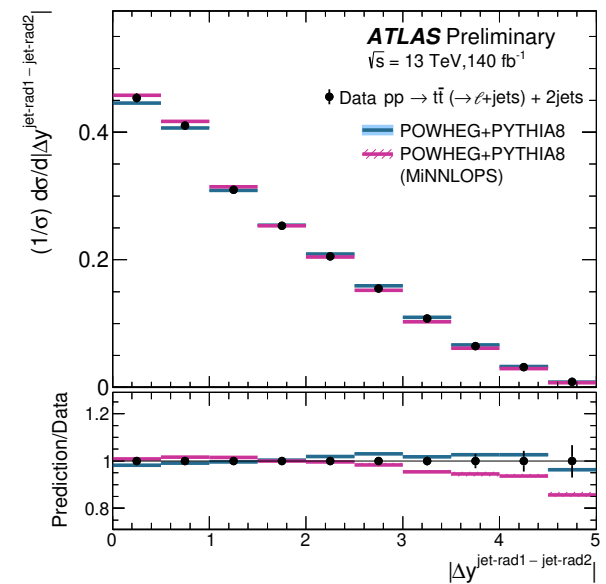
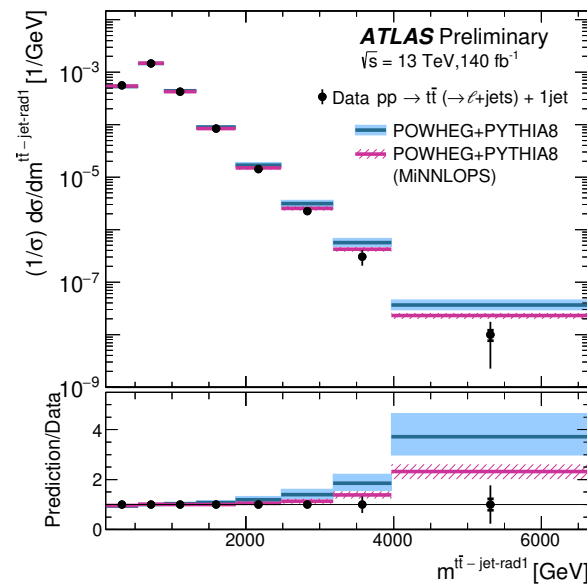
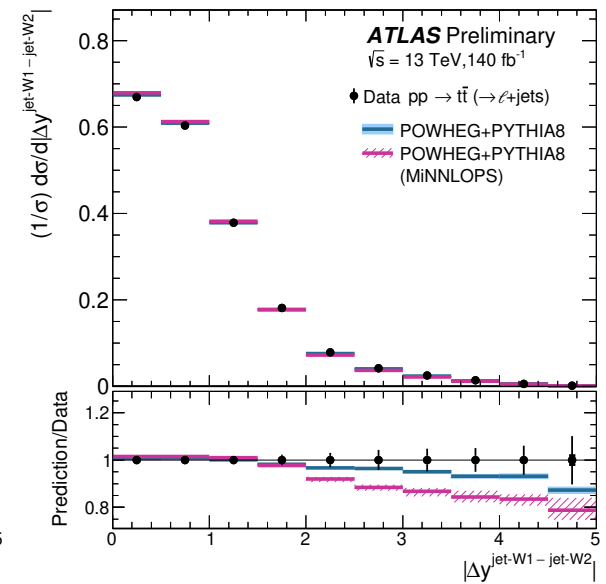
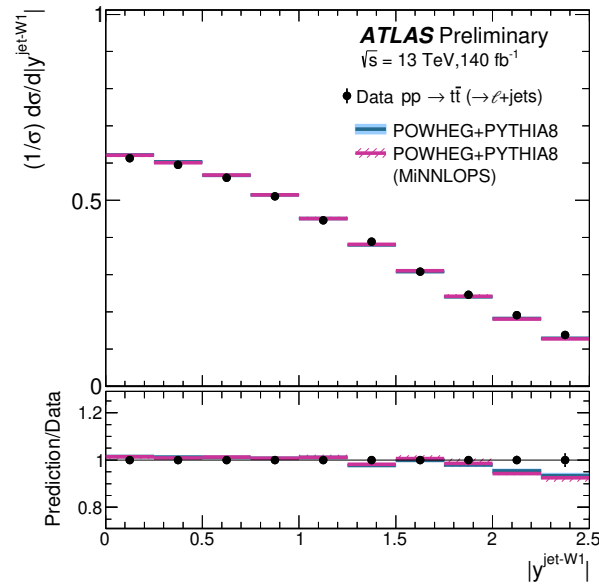




# Results

- Some normalised differential cross sections vs NLO and NNLO:
- ⇒ Reduction of experimental and theoretical uncertainties

⇒ Some regions of phase space are not well described by the predictions tested with the assumptions on the correlations in the theoretical and experimental uncertainties considered



## Summary and conclusions

- **Absolute and normalised differential cross sections at particle level measured for  $t\bar{t}$ (+jets) production in  $\ell$ +jets decay mode using  $140 \text{ fb}^{-1}$  of ATLAS data at  $\sqrt{s} = 13 \text{ TeV}$**
- **Jet angular correlations, jet transverse momenta and invariant masses in the  $t\bar{t}$  inclusive,  $t\bar{t} + 1 \text{ jet}$  and  $t\bar{t} + 2 \text{ jets}$  channels were measured**
- **Characterization of the kinematics of the two jets forming the top-had:**
  - the measured  $p_{\text{T}}^{\text{jet-W1}}$  cross section has a harder spectrum than that of  $p_{\text{T}}^{\text{jet-W2}}$
  - the measured  $|y^{\text{jet-W1}}|$  and  $|y^{\text{jet-W2}}|$  cross sections have very similar shape
  - the measured  $|\Delta y^{\text{jet-W1} - \text{jet-W2}}|$  ( $|\Delta\phi^{\text{jet-W1} - \text{jet-W2}}|$ ) cross section exhibits a peak around  $|\Delta y^{\text{jet-W1} - \text{jet-W2}}| = 0$  ( $|\Delta\phi^{\text{jet-W1} - \text{jet-W2}}| = 1$ )
- **Characterization of the dynamics of the first and second emissions:**
  - values of  $m^{t\bar{t} - \text{jet-rad1}}$  ( $m^{\text{jet-rad1} - \text{jet-rad2}}$ ) up to 5.3 TeV (4 TeV) are measured
  - the measured  $m^{t\bar{t} - \text{jet-rad1}}$  and  $m^{\text{jet-rad1} - \text{jet-rad2}}$  cross sections decrease by more than five orders of magnitude in the measured range

## Summary and conclusions

- **Characterization of the topology in events with hard QCD radiation:**
  - differences in shape of the measured cross sections for rapidities and angular correlations for jet-rad1/2 wrt those measured for jet-W1 indicate that the first and second emissions tend to be more isotropic in rapidity than the jets forming the tophad
  - the measurements also show that first and second emissions have higher probability of arising far from the toplep and that there are more events with a gluon emission back-to-back with the jets forming the toplep
  - the measured features indicate that the second hard emission tends to be close in rapidity to the first emission and that there is a weak dependence of the difference in  $\phi$  between the first and second emissions
- **NLO QCD predictions describe well the shape of the angular observables, but the transverse momenta and invariant masses are described in general only by SHERPA**
- **NNLO QCD predictions give an improved description of the transverse momentum and invariant mass measured cross sections with smaller theoretical uncertainties**
- **The normalised cross sections (with reduced uncertainties) show there are regions of phase space in which the predictions tested do not describe the data with the assumptions on the correlations in the theoretical and experimental uncertainties considered**